Journal of Theoretical and Applied Information Technology
15th December 2016. Vol.94. No.1

ISSN: 1992-8645 www.jatit.org E-ISSN: 1817-3195

DETECTION OF RING ARTIFACTS IN COMPUTED TOMOGRAPHIC IMAGES

[1]MOHAMED ELOTMANI, [2]ABDELMAJID ELMOUTAOUAKKIL, [3]FRANCOISE PEYRIN, [4]MUSTAPHA AGNAOU

[1]Laboratory of Electronics, Instrumentation and Energy, Department of Physics, Faculty of Sciences, University Chouaib Doukkali, Eljadida, MOROCCO

[2]Laboratory ROSERI, Department of Computer Science, Faculty of Sciences, University Chouaib Doukkali, Eljadida, MOROCCO

[3]Univ Lyon, INSA Lyon, UCBL, Creatis, CNRS 5220, Inserm 1206, 69621 Villeurbanne Cedex, FRANCE

[4]Laboratory of Electronics Instrumentation and Energy, Department of Physics, Faculty of Sciences, University Chouaib Doukkali, Eljadida, MOROCCO

E-mail: [1]elotmani.simohamed@gmail.com, [2]elmsn@hotmail.fr, [3]-francoise.peyrin@creatis.insa-lyon.fr, [4]mostaf_agn@yahoo.fr

ABSTRACT

In X-ray Computed Tomography, ring artifacts can be caused by imperfect elements in a detector or also by defects or impurities in the scintillator's crystals. The artifacts appear on Computed Tomographic images as concentric rings superimposed on the images of the structures being scanned. The presence of such artifacts significantly complicates the post processing techniques such as noise reduction, binarization, or segmentation of image information. The efficacy of these techniques depends on the consistency of the method of classification and detection of ring artifacts. In this paper we present a simple, fast and efficient method to detect ring artifacts on Computed Tomographic images in the Polar domain.

Keywords: *Computed Tomography, Ring Artifact, Strip Artifact, Polar Coordinates, Post processing*.

1. INTRODUCTION

The x-ray images used to generate the tomographic images are generated first by exposing the patient to a fan-shaped x-ray beam and then detecting the projected image on a thin semicircular, digital x-ray detector. The patient is placed between the source and the detector, which is configured with its geometric center located at the x-ray source. Each image is an x-ray projection of a very thin transverse slice of the body. To collect the multitude of x-ray projections necessary to generate a Computed Tomographic (CT) image, both the x-ray source and the detector spin around a patient within a supporting gantry. While the source and the detector rotate, images are collected and stored. As in a traditional x-ray, the signal levels in the image slice represent the relative radio density of the patient along a line from the x-ray source to the corresponding pixel location.

The tomographic CT images are corrupted by concentric rings called ring artifacts. These ring artifacts change width and intensity depending on the phenomenon they are generated with such as:

- Detector's defective elements such as dead pixels in a CCD with nonlinear responses.
- Incoming intensity creating sharp rings in the reconstructions of width of one or two pixels [1].
- Anomalies in screen scintillator (scratches, dust...) [2].
- Beam instabilities provoking wider and less marked rings instead [3,4].
- Other causes arise from monochromator [2] or due to the thermal processes of CCD [5].

In particular, we intend to apply our method to synchrotron micro CT images obtained at the ESRF. The European Synchrotron Radiation Facility (ESRF) is the most powerful synchrotron radiation source in Europe. A synchrotron is a

ISSN: 1992-8645 www.jatit.org E-ISSN: 1817-3195

stadium-sized machine that produces many beams of bright X-ray light. Each beam is guided through a set of lenses and instruments called a beamline, where the X-rays illuminate and interact with samples of material being studied. CT images produced by ESRF are often corrupted by ring artifacts (figure 1).

The presence of these ring artifacts on images corrupts the pixel's gray values and makes it difficult to use the image whether in reducing noise or in realizing segmentations [6].

These artifacts are corrected by different techniques:

- The Flat-Field correction [1]. It consists in acquiring background images without sample before and after the acquisition of the desired sample and sometimes during acquisition. These background images contain answers to non-uniformity of incident X-rays, scintillator and detectors. The artifacts are not completely eliminated when different sensors have different response functions [7, 8 & 10].
- Mask the effect of varied responses of different detector elements by moving detector array during the acquisition [9].
- Image processing techniques that identify the ring artifacts and remove them by using filtering and smoothing techniques [6, 11, 13]. These image processing techniques are applied directly to the sinogram or to the reconstructed image.

The first and the second correction techniques are based on experimental measures; therefore, they are limited by various parameters such as the nature of the ring artifact and variability of various acquisition organ responses. It is difficult to remove all ring artifacts and have most reconstruction quality solely by using those experimental techniques. Consequently we need to integrate the image processing techniques to exceed the limits of correction of experimental methods.

The third technique presents the image processing methods. These methods perform image processing on sinogram image formed by the acquired projections, or perform image processing on the CT image after reconstruction from the sinogram. They improve the quality of ring artifact removing methods,

The main objective of this research work is to develop efficient method to identify and detect the ring artifacts in a CT image. A precise identification of the ring artifacts allows improving the ring artifacts removing methods. Our method was tested on CT-images and the experimental results proves that the detection of ring artifacts is global as discussed in section 4.

2. LITERATURE REVIEW

In the literature, there are two types of image processing methods:

- A first type of methods known as sinogram processing methods, which consists in applying image processing to the sinogram image as proposed by [3, 4, 5, 12, 15-26]. The method presented in [3] is based on wavelet and Fourier combined transformation applied to the corrupted sinogram. This combined wavelet-FFT filter represents a powerful approach for a large variety of stripe artifact removal problems. But the authors conclude that, the presence of few stripe artifacts induces to a small loss of sinogram information. This lost affects the CT image, reconstructed by using the sinogram information. The article [5] is based on the theory of inverse and ill-posed problems. The authors minimize the impact of the smoothing Tikhonov's functional used with conjugate gradient method. This minimization is still limited to eliminate all ring artifacts. [12, 15] calculate the sum of corrupted sinogram rows, and smooth the curve of this sum. These two methods use normalization procedure that is weak to eliminate the varying intensity ring artifacts [15, 19-21]. In [17], authors detect the positions of corrupted pixels by using the flat-field image. This method is effective to remove the ring artifacts from a 3-D CBVCT image, but it is weak to remove ring artifacts from micro-CT image [1]. [18] shows that the method is effective for correcting ring artifacts having constant intensities independently of the rotation angle. The method in [19] is based on the center weighted median filter applied on sinogram rows, also, [20] applies a morphological filter, when [23] applies the WMA/VWMA filters. These three methods [19, 20, 23] cannot suppress effectively the ring artifacts with variable intensity. Authors in [21] create a sub-sinogram, where they exploit the polyphase concept to locate the strip artifacts of the sonogram. This method is adapted for the strong ring artifacts.
- The second type of methods known as post processing methods, apply image processing on the CT image after reconstruction, as proposed in [6, 26-28, 30]. In [6] authors transform the CT image to the polar geometric plane, and then they extract the template vector of the stripe

Journal of Theoretical and Applied Information Technology
15th December 2016. Vol.94. No.1

ISSN: 1992-8645 www.jatit.org E-ISSN: 1817-3195

artifacts from the polar CT image. This method uses five morphological operations: thresholding, dilatation, masked erosion, erosion and masked dilatation to get a binary image that serves as ROI to correct the ring artifacts. The methods in [26, 27] are based respectively on median and mean filters applying in different geometric planes (Cartesian coordinates and polar coordinates). Authors in [26] show that the application of the filters in polar coordinates is more effective than the application of the same filters in Cartesian coordinates. However, performing the difference between the median filtered image and the thresholded image is not sufficient to identify low intensity ring artifacts.

The result of these image processing methods is a corrected CT image which is supposed to be free of ring artifacts, but none of the image processing methods is appropriate to correct all ring artifacts as it is showed by the comparative study part in the article [1].

The weakness of these methods to eliminate all ring artifacts is due to the variety of the ring artifact aspects, e.g., ring artifacts with varying intensity, ring artifacts near to/far from the center of the CT image, ring artifacts in micro-CT image, ring artifacts superposed near to the edges of different contrast background. For example, methods presented in [3, 6, 26, 27] are weak to eliminate varying intensity ring artifacts. Furthermore, these image processing methods, often leads to distortions in the corrected image; it requires more precise filtering techniques to avoid treating appropriate pixels as artifact pixels, causing Data loss.

The performance of correction methods depends on the efficiency of classifying and detecting artifacts. This research paper proposes a new method that consists in transforming ring artifacts into a strip artifact, by transforming image from Cartesian coordinates to polar coordinates [14] that are more easily to study and then we proceed to detect all pixels of all aspects of ring artifacts. Such detections will subsequently be used to make local and adaptative correction methods on original image to eliminate ring artifacts independently of their aspects, and avoid inducing blurring or other processed artifacts in the outcomes.

Thereafter, we use following notations:

- f(x,y) is the original CT image corrupted by ring artifacts.
- g(r,theta) is the polar image obtained after transforming f(x,y) from Cartesian coordinates to polar coordinates.

3. MATERIEL AND METHOD

In original CT image f(x,y), the artifact pixels are grouped in the form of a ring. In polar CT image g(r,theta), the artifact pixels are grouped in the form of strips. In this paper, the pixels forming ring or strip artifacts will be called artifact pixels. The detection of Artifact pixels is simple and better in the polar domain. After polar transformation, each ring artifact in CT image f(x,y), becomes a strip artifact in polar CT image g(r,theta), with the same width and grayscale.

In this work, we propose a new strip detection scheme that detects strips in polar CT image

As an illustration, figure 1 shows a CT image f(x,y) taken at ESRF (European Synchrotron Radiation Facility) [4], corrupted by ring artifacts and the polar CT image g(r,theta) after transforming in polar domain, we can see clearly that rings in f(x,y), become strips in g(r,theta).

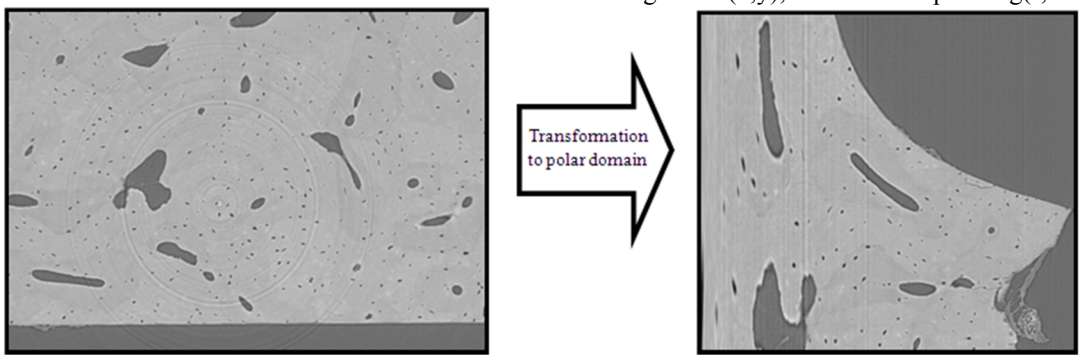

Figure 1 : Image in the left shows a CT image f(x,y)corrupted by ring artifacts in Cartesian coordinates. Image in the right shows polar CT image g(r,theta) that represent f(x,y) in polar domain. g(r,theta) is corrupted by strip artifacts.

ISSN: 1992-8645 www.jatit.org E-ISSN: 1817-3195

Subsequently, the artifact pixel detection will be in polar domain by exploiting properties of strip artifacts in polar CT image. We will study impacts resulting of strip artifact properties.

2.1 The Impact of the Artifact pixel in polar CT image g(r,theta)

A strip creates vertical discontinuity on polar CT image as shown in figure 2-a, in the same figure, a zoomed part of a strip is represented in the red frame, this shows that strip artifact is divided into 2 equal width bands, one band with grayscale values which is darker than the surrounding area, another band with grayscale values which is clearer than the surrounding area.

The impact of a strip artifact is divided into two bands that we called a dark band and a clear band:

- Dark band: artifact pixels belonging to this band are subject to a decrease of their intensity values. Those pixels appear darker than other pixels.
- Clear band: artifact pixels belonging to this band are subject to an increase of their intensity values. Those pixels appear clearer than other pixels.

As an illustration, figures 2-b/c/d/e, show different plots of g(r,theta) when theta is constant and r varies in different intervals that contain artifact pixels. In other words, these plots show intensity values (grayscale level) of selected parts from different lines in the polar CT image.

Plots in figure 2 show also the oscillation (intensity variation) caused by the presence of a strip artifact in a polar CT image area. We note that the variation of intensity values in artifact pixels is higher than the variation of intensity values in surrounding appropriate pixels; as illustrated in figure 2-b, the variation of intensity values in artifact pixels looks like :

- A brief overshoot in the plot of g(r,theta) caused by artifact pixels of the dark band.
- A brief undershoot in the plot of g(r,theta) caused by artifact pixels of the clear band.

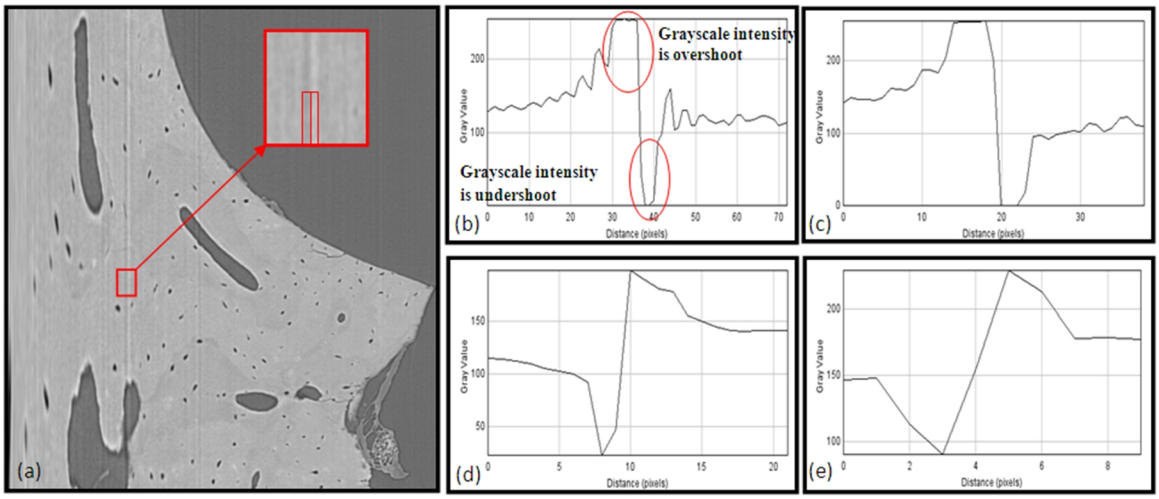

Figure 2 : Image (a) present the Polar CT Image corrupted by strip artifact; Images (b), (c), (d), (e)- present profile plots of different image lines corrupted by artifact.

The idea is to use this overshoot and undershoot of intensity values as a strip artifact property. It is to assume that any serie of artifact pixels presents local minims, shown as grayscale intensity undershoot in plots 2-b/c/d/e or local maxims, shown as grayscale intensity overshoot in plots 2-b/c/d/e. This property is not only specific to artifact pixels but can also characterize some exceptional appropriate pixels.

It will be easy to use thresholding to determine strip artifact oscillations if strip artifact intensity are uniform, which is not the case in corrupted CT images.

Thereafter polar CT image will be transformed in order to make the strip artifact intensities uniform, by a maximal broadening of artifact, to make clearly visible, inter alia, all Strip artifacts.

The transformation consists in decreasing grayscale intensity of the artifact pixel to zero value (dark pixel) if the artifact pixel belongs to artifact pixels presenting local minims, and increasing grayscale intensity of artifact pixel to a value of 255 (white pixel) if the artifact pixel belongs to artifact pixels presenting local maxims. After this transformation, the result image will be called Mg(r,theta) that represents the polar CT image

ISSN: 1992-8645 www.jatit.org E-ISSN: 1817-3195

g(r,theta) after the variation of some pixel intensities including artifact pixel intensities. The changed pixels will be called "marked pixels".

Figure 3-c shows the polar CT image with marked strip artifacts that have the same grayscale intensity. Also, we can see change in grayscale appropriate pixels, due to marking appropriate pixels as artifact pixels.

To keep only strip artifacts marked, we need to add another property which is the linearity of artifact pixels.

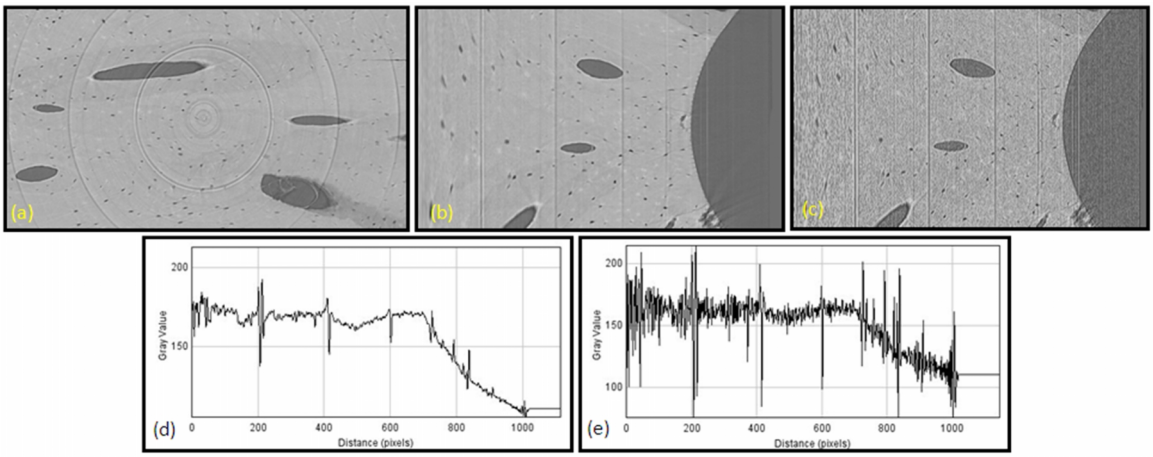

Figure 3: (a)- CT image superimposed by ring artifacts f(x,y); (b)- CT image in polar domain g(r,theta); (c)-Image Mg(r,theta) obtained after marking artifact pixels in g(r,theta); (d)- s(r)=sum(g(r,theta)) sum curve of all gray values of each column of g(r,theta); (e)- sa(r)=sum(Mg(r,theta))sum curve of all gray values of each column of Mg(r,theta)

2.2 The Impact of Strip artifact linearity in Marked polar CT image Mg(r,theta)

After marking artifact pixels, by unifying their grayscale intensities, we are using linearity property of these artifact pixels that form strip artifacts.

At first, in image g(r,theta) we proceed to sum the grayscale pixel values of each column.

$$s(r) = \text{sum}(g(r,\text{tetha})) \quad (1)$$

The Plot of s(r) shown in figure 3-d allows to visualize strip artifacts position 'r' in polar CT image [12]. In s(r), strip artifact positions (columns) correspond to local minima and maxima positions in plot of s(r). This proceeding shows weakness to detect low intensity strip artifacts.

Next, we use same proceeding (sum of the grayscale pixel values of column 'r'), this time in marked polar CT image Mg(r,theta).

$$sa(r) = \text{sum}(Mg(r,\text{theta})) \quad (2)$$

The Plot of sa(r) illustrated in figure 3-e allows to visually determine strip artifacts position 'r', even those with low intensity.

Strip artifacts correspond to the extrema in the plot of sa(r) shown in figure 3-e. Every extremum sa(r) corresponds to a unique position 'r' in the polar CT image.

Till now, the determination of the strip artifacts position from the plot of sa(r), is manual and based on visual check. Even if the determination is manual it shows efficiency to find all strip artifacts.

Thereafter, sa(r) will be transformed to have a stable linear trend and help apply a threshold criterion and finally get an automatic detection of strip artifacts.

2.3 Transforming sa(r)

We note Tsa(r) the transformation of sa(r). Tsa(r) maintains the same oscillations in sa(r), with stable linear global trend. The transformation expressed by the formula below contains the moving average of s(r) that we express as a convolution with a mask filter m, and contains the arithmetic average of sa(r)-s(r) that we express as a convolution with a mask filter M.

$$Tsa(r) = sa(r) - s*m\,(r) - (sa-s)*M(r) \quad (3)$$

Figure 4 shows plots of s(r), sa(r) and Tsa(r). After the transformation, we can see that the overall shape/trend curve of s(r) becomes linear and horizontal in Tsa(r), we see also that all oscillations in s(r) were preserved in Tsa(r).

Journal of Theoretical and Applied Information Technology
15th December 2016. Vol.94. No.1

ISSN: 1992-8645 www.jatit.org E-ISSN: 1817-3195

This new form of Tsa(r) allows us to apply a threshold criterion and get an automatic detection of strip artifacts

Application of two adjustable thresholds, as shown in figure 4, allows determining strip artifacts, depending on their intensities and widths.

In figure 4, threshold 1 is used to detect the dark bands of strip artifacts and threshold 2 is used to detect clear bands of strip artifacts.

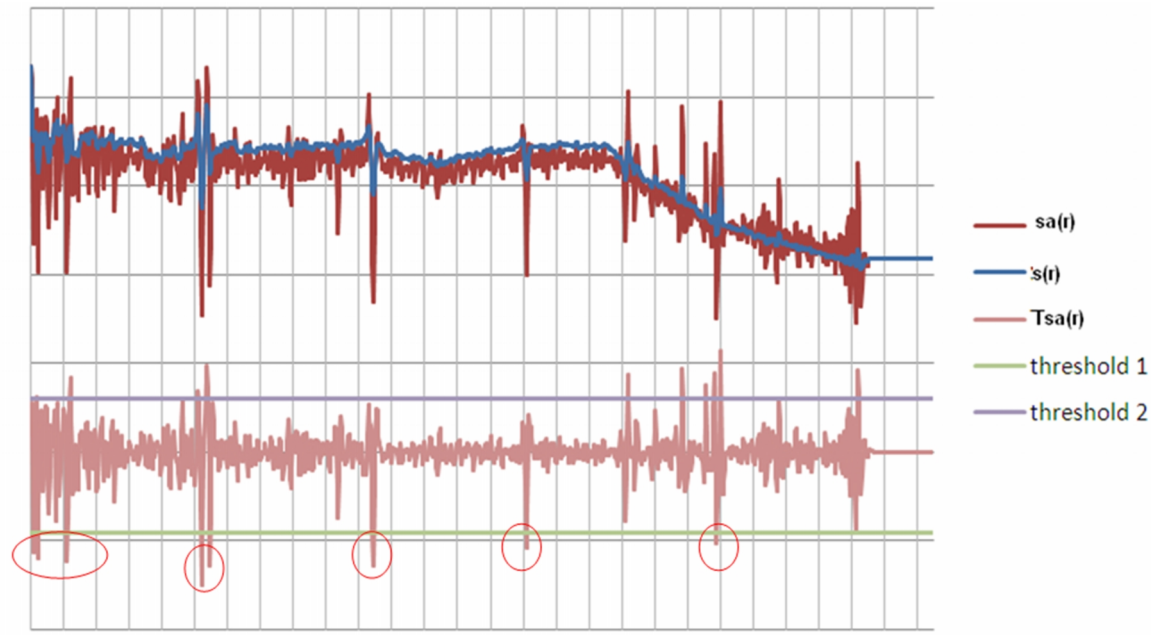

Figure 4 : Plots off s(r), as(r) and Ts(r)

By applying threshold 1, we select local minims (encircled ones in figure 4) that represent dark bands of strip artifacts. In the same way, by applying threshold 2, we select local maxims that represent clear bands of strip artifacts; also, by adjusting threshold 1 and threshold 2, we can detect more dark or clear bands. In some cases, the dark band in a strip artifact is more intense than the clear band; therefore, it is not necessary to detect the clear band in order to correct it.

The used thresholding is flexible and allows detecting more precisely the band (dark or clear) that we judge necessary to correct.

4. EXPERIMENTAL RESULTS

As already mentioned, a good ring artifact correction, must remove all ring artifacts from the CT image, regardless their aspect, thereby, the detection method must locate all these ring artifacts aspects. The different aspects of the ring artifacts that we find in literature are:

- Ring artifact in micro-CT image that affect the quality of microscopic details.
- Ring artifact in the center of the CT image.
- Ring artifact with varying intensity depending of rotation angle: a part of the ring artifact has a high intensity, when another part of the same ring artifact has a low intensity.
- Ring artifacts locate at the edge of two different contrast mediums.

In the following, we apply our method of ring artifact detection to a CT image that contains all the mentioned ring artifact aspects. The left image in Figure 5 shows a micro-CT image of a human core sample, with a pixel size of 1.4µm. we can see in that micro-CT image, ring artifacts in the center, ring artifacts with varying intensity and ring artifacts at the edges of high contrast and low contrast mediums, we see also, ring artifacts with unchanging high/low intensity.

The evaluation criteria is based on how is the method of detecting is efficient to locate all these ring artifacts aspects. In our case, we visually judge the quality of detection because we haven't a corrected image resulting from an image processing, on which we apply objective indices as the conventionally used peak signal-to-noise ratio (PSNR).

ISSN: 1992-8645 www.jatit.org E-ISSN: 1817-3195

To evaluate the result of the ring artifact detection, we must evaluate if the detected ring artifacts using our method really exist in the CT image.

In first we create a binary mask to high light the detected ring artifacts and to better appreciate the efficiency of our detection method, we used a binary mask to the polar CT image. This mask makes black the detected artifact pixels that belong to the dark band of the strip artifact, and it makes white those that belong to the clear band of the strip artifact. The mask has no effect on the original pixels of the polar CT image. After applying the mask, we obtain a polar CT image with "black and white marking" of strip artifact pixels; thereafter we transform the polar CT image from the polar coordinate to Cartesian coordinate to have a CT image with black and white marking ring artifacts. In figure 5, the image in the right side shows the micro-CT image containing the different ring artifact aspects after applying the detection and the binary mask adjusted to chosen thresholds.

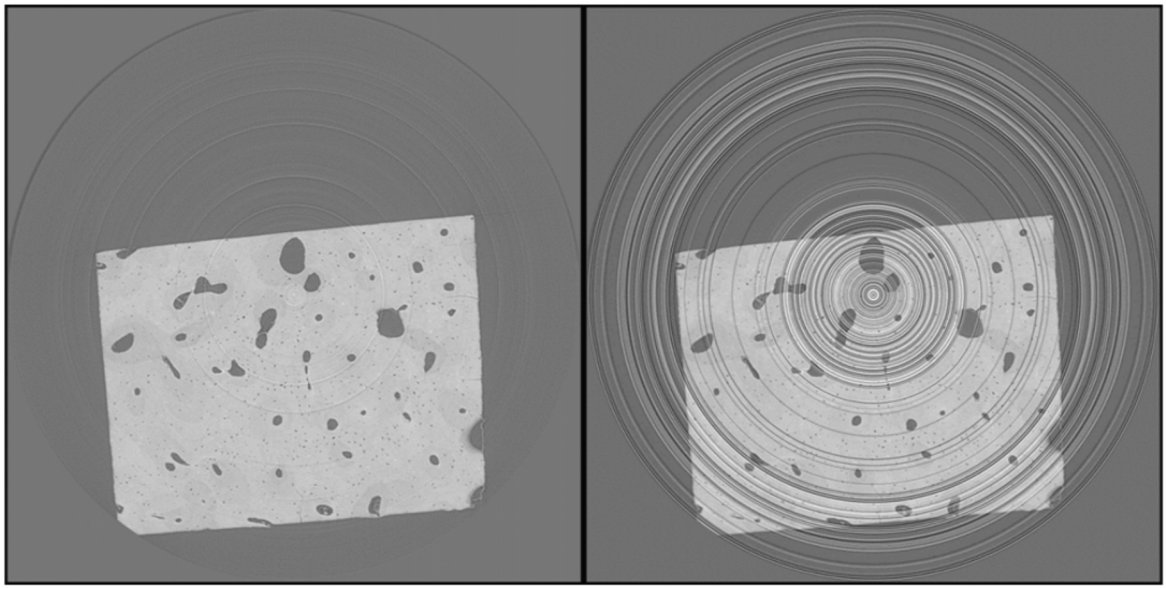

Figure 5 : Original CT image before (left) and after (right) detecting and marking ring artifacts

Figure 5 shows the original CT image corrupted by ring artifacts and the resulting image after applying our method that marks ring artifacts. The threshold adjustment applied to detect artifacts is choosen to show ring artifacts regardless of their width and intensity.

The image after the detection puts in evidence all ring artifacts, including the one in the center of the micro CT-image.

To better see the quality of the detection, we proceed to a visual comparison of a central region of the CT image, where we are applied a detection and a marking of ring artifacts only on a quarter of the selected region. After zooming, the result is shown in figure 6.

Figure 6 above shows the central region of the micro-CT image, on which we applied our detection and marking method only in the top right quarter. It also shows that the ring artifacts which we see in the appropriate regions of the CT image have been marked in the top right quarter.

A simple quantitative comparison in the figure 6 consists in manually counting the ring artifacts that we see, and compare the manually counted number N_m to the number of the detected ring artifacts N_d. We find that $N_m = 78$ when $N_d = 66$, therefore, in figure 6, we have detected 84% of the existed ring artifacts, knowing that we can detect more ring artifacts if we vary the threshold already selected.

We notice that our method has succeeded the detection of ring artifacts on the center, when the other methods in [17, 26] failed. These methods fail to remove ring artifacts in the center of the CT image, which is also the center of the ring artifacts, because in the center of the image ring artifacts follow each other and they are very close, so most of the CT image details are lost in the center of the image.

The methods in [17, 26] use the neighboring pixel grayscale values to locate the ring artifacts, in the center, most of the neighboring pixel grayscale values are corrupted, so the ring artifact location and correction fail. The strength of our method is the precise definition of the ring artifact in 3.1

Journal of Theoretical and Applied Information Technology
15th December 2016. Vol.94. No.1

ISSN: 1992-8645 www.jatit.org E-ISSN: 1817-3195

which allow us to define a ring artifact without using the appropriate pixel grayscale values.
It was noted that the intensity of the ring intensities in the micro-CT image shown in figure 6 are low, this has enabled us to test the precision of our method and confirm that the quality of detecting low intensity artifact by making threshold is more rigorous.

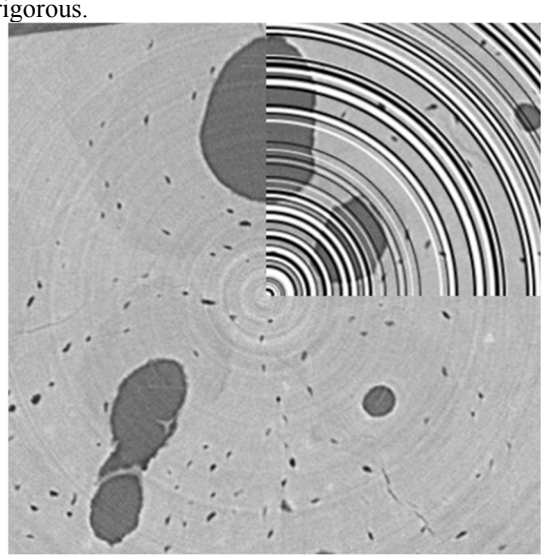

Figure 6 : zoomed central region of the CT image that contains low intensity ring artifacts

The detection of varying intensity ring artifacts is also experimented, and the result is shown in figure 7. This figure present a part of the original micro-CT image that contains two ring artifacts with varying intensities depending on the rotation angle, these two ring artifacts are detected and marked by the binary mask as shown in the tight image of the figure 7.

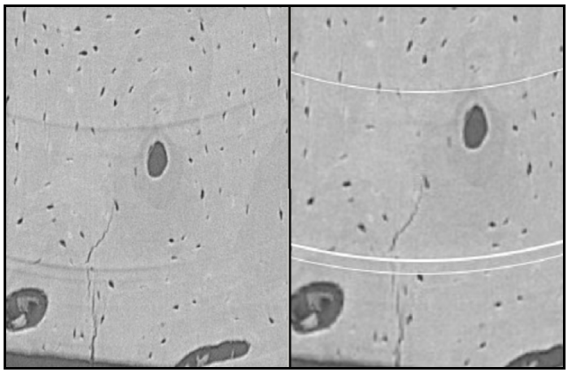

Figure 7: the left image shows zoomed part of the original image that contains three varying intensity ring artifacts and the right image that shows the binary mask applied on the original image with marking the three ring artifacts.

It is clearly proved the efficiency of our method to detect the varying intensity ring artifacts when the methods in [12, 15, 19, 20, 23] fail to detect and remove these artifacts.

The problem of detection varying intensity ring artifacts is the same of detection low intensity ring artifacts, because when we compute the sum curve of the corrupted image as in [12, 15], the sum value of the row that contains low intensity stripe artifacts is close to the sum value of an appropriate row without artifacts, So we cannot distinguish between a row with artifacts and a row without artifacts based on the sum curve technique.

In our method we "amplify" the grayscale value of suspected pixels by decreasing and increasing the original grayscale pixel values, to make uniform the pixel values in the same ring artifact presented in 3.1.

In regards to some ring artifacts at the edges of two contrast objects as shown in figure 8, the ring artifact are more shown as the black circle when it is in the clear part of the image, but when the ring artifact is in the dark part of the image, it is more shown as a white circle.

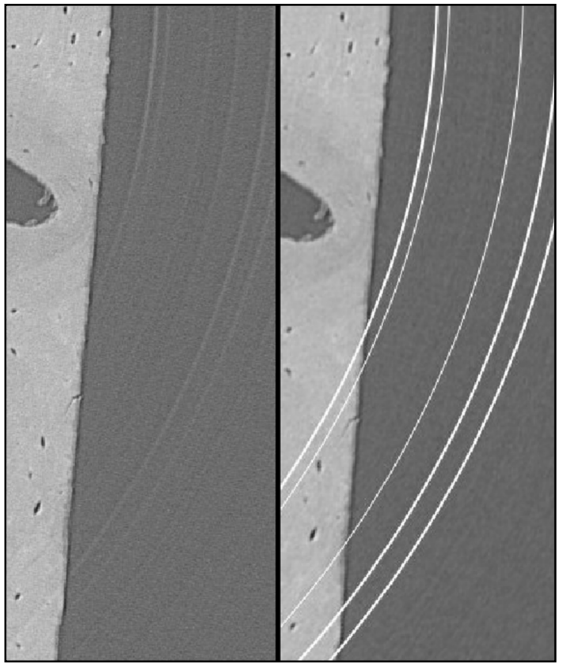

Figure 8:

The methods as [22] of removing ring artifacts at the edges of two different contrast mediums, must detect the black circle in the clear part of the CT image, and detect also the white circle in the dark part of the CT image. This is two opposite definition of the same ring artifact.

The ring artifact as defined in 3.1, shows that it contains two sides, the undershoot side and the overshoot side. The undershoot side is more

ISSN: 1992-8645 www.jatit.org E-ISSN: 1817-3195

visible in the clear part of the CT image when the overshoot side is more visible in the dark part of the CT image. This description of the ring artifact allows us to better detect these rings regardless of the medium.

Our detection method is very efficient to found all ring artifacts. It also allows the user to choose the degree of precision in detection.

Our method to detect ring artifacts was applied on different CT images produced in ESRF and corrupted by ring artifacts. These rings have different intensities, widths and aspects. So we make different detection with different threshold adjustments to see what our proceeding is capable to found; thereafter we present detection in original CT images in Cartesian domain with different threshold adjustment.

We have tested our method with different threshold adjustments applied on six different CT images produced in ESRF. The figure 9 below shows these results that we obtained. Also, it shows that we can apply different level of detection for the same CT image.

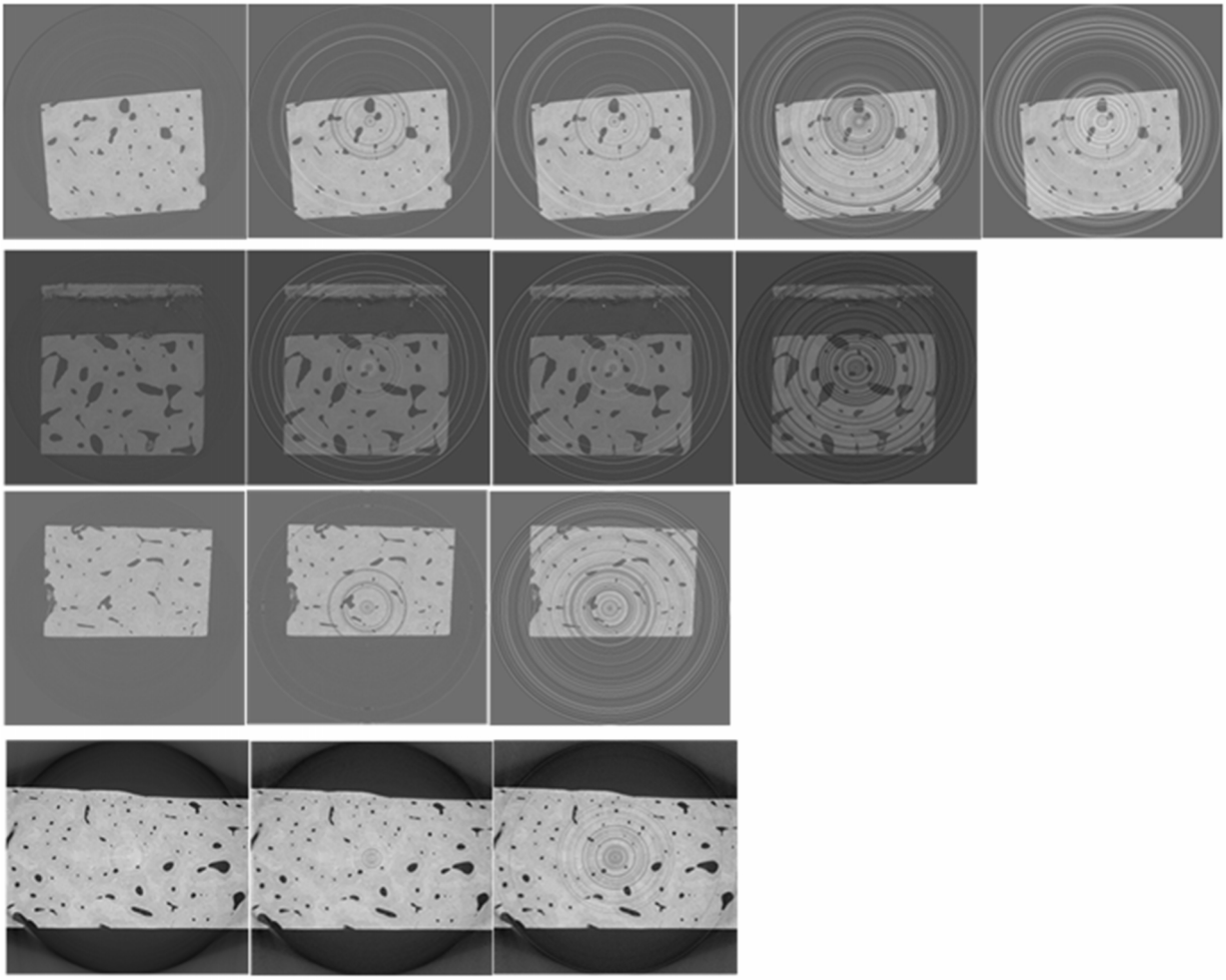

Figure 7 : In the left column the original CT images produced in ESRF, the other images shows marking ring artifacts with different threshold adjustment

5. OPEN RESEARCH ISSUES

The methods used in the literature can be improved to better correct the ring artifacts:

- In [3], the method is weak to suppress completely the varying intensity ring artifact. This weakness can be enhanced by adapting the wavelet-Fourier filter to take into consideration the low values of the frequency that correspond to the low intensity parts of a ring artifact by considering the variation of the gray scale level of the strip artifact when the thresholding is applied after the wavelet-Fourier transformation.

ISSN: 1992-8645 www.jatit.org E-ISSN: 1817-3195

- The ring corrections using homogeneity test method presented in [6] and the ring artifact correction in polar coordinates method presented in [26] fail to completely correct the ring artifacts especially the varying intensity rings that need a pre-correction before applying the two methods.
- The algorithm used in [17] to reduce ring artifacts can be enhanced by using the information of the neighborhood pixels of the artifacts.

6. CONCLUSION

The adaptability and the precision of our detecting method allow users to choose the precision of detection, to correct all or some ring artifacts that they judge necessary for our CT image treatment. The correction then will be easier and more precise.

This method presents a base for many local correction methods to be explored in tomography domain, without perturbing CT image information.

The method allows detecting artifacts but it cannot classify them by their types. This classification is the subject of our future work. When the classification is completed, this would then make it possible to develop correction methods that correspond to each type of ring artifacts, and, thereafter, build a complete method that eliminates all type of ring artifacts.

7. REFRENCES

[1] Emran M Abu Anas, Jae G Kim, Soo Y Lee, Md. K Hasan: Comparison of ring artifact removal methods using flat panel detector based CTimages BioMedical Engineering OnLine 2011, 10:72 10.1186/1475-925X-10-72

[2] Titarenko V, Bradley R, Martin C, Withers P, Titarenko S: Regularization methods for inverse problems in X-ray tomography. Proc. SPIE 2010, 7804:7804z-1-10.

[3] MÄunch B, Trtik P, Marone F, Stampanoni M: Stripe and ring artifact removal with combined wavelet-Fourier Filtering. Opt. Express 2009, 17(10):8567-8591.

[4] Raven C: Numerical removal of ring artifacts in microtomography. Rev. Sci. Instrum. 1998, 69(8):2978-2980.

[5] Titarenko S,Yagola A: Ring artefact suppression in realtime X-ray tomography. Moscow University Physics Bulletin 2010, 65:65-67.

[6] Sijbers J, Postnov A: Reduction of Ring Artifacts in High Resolution Micro-CT Reconstructions. Phys. Med. Biol. 2004, 49(14):247-253.

[7] G. T. Herman, Image Reconstruction from Projections – The Fundamentals of Computed Tomography, Academic Press New York, 1980.

[8] Antoine C., Nygard P., Gregersen O. W., Holmstad R., Weitkamp T., Rau C., 3D images of paper obtained by phase-contrast X-ray microtomography: image quality and binarisation, Nuclear Instruments and Methods in Physics Research Vol. 490, No. 1, pp. 392-402(11), Sep. 2002.

[9] Davis G.R., Elliott J.C, X-ray microtomography scanner using time-delay integration for elimination of ring artifacts in the reconstructed image, Nuclear Instruments and Methods in Physics Research A, Vol. 394, No.1, pp.157-162(6), July 1997.

[10] Vidal F.P., Letang J.M., Peix G., Cloeten P., Investigation of artefact sources in synchrotron microtomography via virtual X-ray imaging. Nuclear Instruments and Methods in Physics Research B 234 pp.333–348 2005.

[11] Cai.Z,Ringing Artefact Reduction Using Adaptive Averaging Filtering," Proc. ISCE, UK, June, p.156–159, 2004.

[12] M.Boin and A. Haibel, Compensation of ring artefacts in synchrotron tomographic images, Opt. Express Vol.14, Issue 25, pp.12071-12075, 2006.

[13] Guifang DUAN, Yen-wei CHEN, Xianhua HAN, Akinori FUJITA, Ken HIROOKA and Yoshihiro UENO, Reduction of Ring Artifacts in Cone-Beam CT images, IEICE Technical Reports, Vol.107, No.461, pp.227-233, 2008.

[14] R Jagadeesh Chandra Prasad et al, PoWer: Polar Wavelet-Gaussian Filter for ring artifact suppression in CT Imaging Systems International Journal of Computer Science & Communication Networks,Vol 1(2), 186-195, ISSN:2249-5789, 2011

[15] Ketcham RA: New algorithms for ring artifact removal. In Proc. SPIE, Volume 6318 2006:63180O-1-7.

[16] Rivers M: Tutorial Introduction to X-ray Computed Microtomography Data Processing. http://www.mcs.anl.gov/research/projects/X-ray-cmt/rivers/tutorial.html, University of Chicago 1998.

[17] Tang X, Ning R, Yu R, Conover D: Cone beam volume CT image artifacts caused by defective cells in x-ray °at panel imagers and the artifact

ISSN: 1992-8645 www.jatit.org E-ISSN: 1817-3195

removal using a wavelet-analysis-based algorithm. Med. Phys. 2001, 28(5):812-825.

[18] Titarenko S, Withers PJ, Yagola A: An analytical formula for ring artefact suppression in X-ray tomography. Applied Mathematics Letters 2010, 23:1489-1495

[19] Sadi F, Lee SY, Hasan MK: Removal of ring artifacts in computed tomographic imaging using iterative center weighted median filter. Computers in Biology and Medicine 2010, 40:109-118.

[20] Hasan MK, Sadi F, Lee SY: Removal of ring artifacts in micro-CT imaging using iterative morphological filter. Signal, Image and Video Processing 2010. [DOI 10.1007/s11760-010-0170-z].

[21] Anas EMA, Lee SY, Hasan MK: Removal of ring artifacts in CT imaging through detection and correction of stripes in the sinogram. Phys. Med. Biol. 2010, 55:6911-6930.

[22] Anas EMA, Lee SY, Hasan MK: Classification of Ring Artifacts for Their Effective Removal Using Type Adaptive Correction Schemes. Computers in Biology and Medicine 2011, 41(6):390-401.

[23] Ashrafuzzaman ANM, Lee SY, Hasan MK: A Self-Adaptive Approach for the Detection and Correction of Stripes in the Sinogram: Suppression of Ring Artifacts in CT Imaging. EURASIP Journal on Advances in Signal Processing Volume 2011. [DOI 10.1155/2011/183547].

[24] Ming LC, Gordon BM: Ring suppression filter for use in computed tomography systems. United States Patent 1998.

[25] Hamill JJ, Faul DD: System and method for reducing circular artifacts in tomographic imaging. United States Patent 2010.

[26] Prell D, Kyriakou Y, Kalender WA: Comparison of ring artifact correction methods for flat-detector CT. Phys. Med. Biol. 2009, 54:3881-3895.

[27] Kyriakou Y, Prell D, Kalender WA: Ring artifact correction for high-resolution micro CT. Phys. Med. Biol. 2009, 54:N385-N391.

[28] Titarenko S, Titarenko V, Kyrieleis A, Withers PJ: A ring artifact suppression algorithm based on a priori information. Applied Physics Letters 2009, 95:071113-1-3.

[30] Journal of Theoretical and Applied Information Technology 15th December 2012. Vol. 46 No.1 *REDUCING THE GAUSSIAN BLUR ARTIFACT FROM CT MEDICAL IMAGES BY EMPLOYING A COMBINATION OF SHARPENING FILTERS AND ITERATIVE DEBLURRING ALGORITHMS* **1** ZOHAIR AL-AMEEN, 1 GHAZALI SULONG, 2 MD. GAPAR MD. JOHAR